Wavelike Eddies in a Turbulent Jet

Y.Y. Chan*
National Research Council of Canada, Ottawa, Canada

Experimental and theoretical studies of the wavelike disturbances in an axisymmetric turbulent jet are presented. It is demonstrated that the jet can support a helical wave train with azimuthal mode equal to or greater than unity in addition to the plane wave mode. The disturbance wave grows rapidly along the jet to a maximum and then decays gradually further downstream for three modes considered, $m=0$, 1, and 2. The disturbance waves of all modes are well modeled by a wave theory with the local properties of the wave described by a linear stability solution of a divergent shear flow. The nonlinear development of the wave along the jet is calculated by an energy integral method. The predicted results are in good agreement with the experimental data.

Nomenclature

b = parameter, shear layer thickness
c = complex number, $c=\beta/\alpha$, Eq. (13)
k = turbulent kinetic energy, total wave number
L = dissipation length
m = azimuthal wave number
p = pressure
q = wave kinetic energy
Q = wave amplitude
R = radius of jet nozzle exit
t = time
u,v,w = velocity components in x, r, ϕ directions, respectively
x,r,θ = cylindrical coordinates
y = radial coordinate
α_r = wave number
$-\alpha_i$ = amplification rate
β = circular frequency
δ = shear layer thickness
ϵ = turbulent dissipation
ζ,η = transformed coordinates for x, r, respectively, Eq. (8)
ϵ_t = kinematic eddy viscosity
σ_k = Prandtl number for the turbulent kinetic energy equation, Eq. (7)
ϕ = wave energy dissipation, Eq. (3)
χ = complex function, Eq. (15)

Superscripts

$\overline{\ }$ = time mean values
$\tilde{\ }$ = wave fluctuation
$'$ = turbulent fluctuation

Averaging Process

$\overline{\overline{\ }}$ = time averaged

I. Introduction

THE coherent structure of the turbulence in a free jet has attracted considerable interest in recent years becasue of its functions in the generation of noise from the jet. The orderly structure in a turbulent jet was first recognized by Mollϕ-Christensen in an experimental study of the near pressure field of the jet. By measuring the space-time correlation of the pressure fluctuation, he found that the disturbance (or eddy) was convected downstream for a considerable distance and decayed slowly.[1] A more detailed study of the large-scale eddy motion was given by Crow and Champagne.[2] In their experiment, a disturbance with certain frequency was introduced into the jet and the development of the disturbance along the jet was then followed by measuring the velocity fluctuation. A wave system was found in the jet and the wavelength depended on the forcing frequency and the jet velocity. The amplitude of the wave reached a maximum and then decayed gradually downstream in accordance with Mollϕ-Christensen's observations.

In an experiment, extending Crow and Champagne's measurements, Chan measured the pressure fluctuations inside a jet with external forcing.[3] With a phase-averaging technique and processing the narrow-band filtered signals, he demonstrated clearly the wavelike behaviors of the large-scale eddies. More recently, Lau and Fisher showed the existence of the orderly structure in a jet without forcing, using a novel experimental technique.[4] By locking onto the spikes that appeared rather regularly in the hot-wire signal and taking the phase average, the resulting signal became sinusoidal in shape. This indicated that the large-scale eddies have a wavelike coherent structure. For an axisymmetric jet, the structure of the large-scale eddies can be quite complicated as shown by Fuchs.[5] By taking the space-correlation circumferentially around the jet, he decomposed the power spectra of the fluctuating pressure into Fourier components of azimuthal wave numbers and showed that the first four components dominated. This suggests that the eddies are not only translating as a plane wave along the jet but also spiralling around the jet at the same time. This multimode characteristic in the jet was also observed by Browand and Laufer.[30]

In addition to these representative works, an excellent review of the advance of the subject up to 1974 is given by Davies and Yule.[6] An extensive bibliography is included with the review.

Parallel to the studies of the orderly structure of the turbulent jet the evaluation of the function of the large-scale eddies in the generation of noise from the turbulent jet also absorbed a large amount of research effort. It was pointed out by Mollϕ-Christensen that a coherent structure would radiate acoustic energy more effectively than a random structure.[1] This concept has found its way in a number of jet noise theories formulated in later years. In Lilley's theory, the wave of the shear layer was taken as the solution of the inner source region.[7] In Michalke's expansion theory, the multicomponents of the wave structure were incorporated explicitly in the source function.[5,8] For a supersonic jet both the near- and the far-field of the acoustic radiation were shown by Liu[9,10] and Tam,[11,12] respectively, to be related to the large-scale eddy motions. These theories in high-speed jets were substantiated by experimental measurements of McLaughlin et

Received Dec. 1, 1976; presented as ICAS Paper 76-42 at the Tenth Congress of the International Council of the Aeronautical Sciences, Ottawa, Canada, Oct. 3-8, 1976; revision received April 18, 1977.

Index categories: Jet, Wakes and Viscid-Inviscid Flow Interatctions; Aeroacoustics.

*Senior Research Officer, High Speed Aerodynamics Laboratory. Member AIAA.

al.[13,14] In a less direct manner, relating to the wavelike motion of the large eddies, Laufer et al. proposed that the rate at which these eddies interacted with each other was the primary mechanism of the noise generation in a subsonic jet.[15]

The large-scale eddies in the turbulent jet as observed in the experiments show that their behaviors are very much like a wave train propagating in a shear flow. It is natural to extend Landahl's wave guide theory, formulated to explain the orderly structure in a turbulent boundary layer, to the turbulent free shear flows.[16] Landahl's model has been applied by Hussain and Reynolds to turbulent channel flows with some success.[17] For a turbulent jet, this model has been used by Liu[9,10] for the calculation of the near acoustic field of a two-dimensional jet and by Tam[12] for the acoustic far-field of an axisymmetric jet. More detailed analyses for axisymmetric low-speed jets were given by Morris[18] and Chan[19,20] with emphasis on the turbulent modeling. The calculated development of the large-scale eddies by the wave theory was shown by Chan to be in good agreement with experimental data.[20]

In the present paper we present some new experimental results on the orderly structure of the turbulent jet. In addition to the axisymmetric wave system, we show that a helical wave system with the azimuthal wave number equal to or greater than unity can also exist. The development of these waves of higher modes are shown to be well modeled by the wave theory. This paper deals first with the direct measurements of the helical wave in the turbulent shear layer of the jet. Following that, it is shown how the disturbance waves can be modeled by the stability wave theory, and its nonlinear development along the jet is calculated. The calculated results and the experimental data are then compared and discussed in some detail.

II. Measurement of Helical Wave Development in the Jet

A. Experimental Apparatus and Method

The air jet used in the experiment was generated by the low-speed jet facility of the NAE High Speed Aerodynamics Laboratory. The Facility was carefully designed to provide a jet with low turbulence and low internal noise. The details of the facility are given in Ref. 21. For the present experiment, the internal diameter of the nozzle exit was 5.7 cm. The jet was running with an exit velocity of 76 m/sec nominal and the corresponding Reynolds number of 26×10^4 based on the nozzle diameter.

A schematic drawing of the equipment set-up for the experiment is shown in Fig. 1. Six acoustic drivers were mounted circumferentially around the jet with 60-deg spacing at the nozzle exit to provide periodic forcing at the jet boundary. Each driver unit consisted of a 40-W loudspeaker driver and a converging duct with one end connected to the driver and the other opened to an exit slit 1.3×9 mm. The phase and amplitude of each driver could be adjusted independently. In this experiment, all drivers were tuned to the same frequency with a beat frequency oscillatory, but with a phase advance between each unit of 60 deg in sequence, thus generating an azimuthal mode of $m=1$. Higher modes could be similarly obtained with corresponding phase advances. The forcing amplitude of the drivers was set to 124 dB re. 0.0002 dynes/cm^2 at the exit of the duct with the jet running. The development of the disturbance along the jet was recorded by monitoring the static pressure fluctuation with two Brüel and Kjaer 3.2-mm-diam microphones with bullet head fairings. The pressure signals from the traversing microphones were fed into the narrow-band filters slaved to the forcing frequency. At each position of the traversing probes, the filtered signals were then used to drive the vertical displacement of an oscilloscope. The periodic signal from the oscillator was converted by a stroboscope unit into timing spikes to trigger the oscilloscope intensity modulation at the required phase. Thus, the presence signal oscillating about vertically would be lit up as a bright spot only at the time triggered by the stroboscope. The probes were then moved to another position, and the process was repeated until a continuous trace was obtained and recorded by a memory scope or an open-shutter camera. This intensified trace now displayed the spatial variation of the pressure signal at a fixed phase (or time as defined in Fig. 1). The rms value of this signal was recorded in parallel on a level recorder. Traverses were made with two microphones mounted one nozzle diameter apart symmetrically about the center-line of the jet. This technique of experiment is similar to that described in Ref. 3 for the measurement of plane waves development in a jet.

B. Experimental Results and Discussion

With this experimental set-up it was quite easy to establish that the jet did support helical wave systems. Some typical results of the pressure signature displayed spatially are shown in Fig. 2. For the first case, the drivers were set to generate a mode of $m=1$, the pressure waves recorded by the traversing microphones shown in the picture are exactly 180 deg out of phase. For the second case, the drivers were set to generate the $m=2$ mode and the pressure waves are now in phase. In both cases, the waves amplify rapidly and then decay farther downstream, with characteristics similar to those of the plane waves.[3] The present experimental results verify the theoretical analysis of Batchelor and Gill that for an axisymmetric jet with a "top-hat" velocity profile, such as the one near the nozzle exit, all disturbances of $m\geq0$ will be amplified.[22]

The wavelength of the helical wave in the direction of the jet x can be measured directly from the oscilloscope traces.

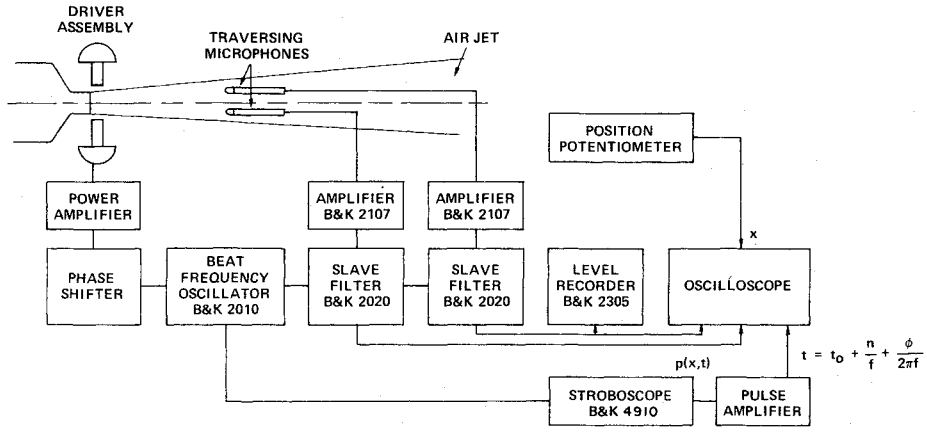

Fig. 1 Schematic diagram of instrumentation for the experiment.

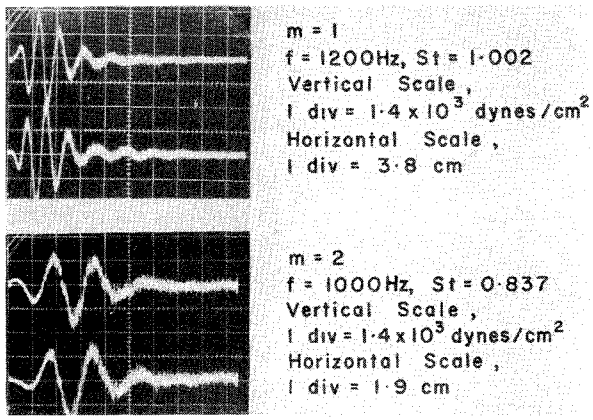

Fig. 2 Spatial pressure waves along the jet for modes $m = 1$ and 2.

Because of the thicknening of the shear layer along the jet, the wavelength increases gradually in the downstream direction. The distance between the second and the fourth zero crossings of the wave form is considered as the average value of the wavelength. The total wave number along the direction of the wave helix is calculated from the wave number in the x direction α

$$kR = \{m^2 + (\alpha R)^2\}^{1/2} \quad (1)$$

where m is the azimuthal wave number and R the radius of the nozzle. The total wave number k as a function of Strouhal number fD/U based on the forcing frequency f, the nozzle diameter D, and the jet exit velocity U, is shown in Fig. 3a for both the $m = 1$ and $m = 2$ modes. Results for the $m = 0$ mode, taken from Ref. 3, are also plotted for comparison. For the same Strouhal number, the wave number increases as the mode increases. The phase velocities of the wave in the direction of the helix are shown in Fig. 3b. Results of the $m = 0$ mode are also shown for comparison. Opposite to the trend of the $m = 0$ mode the phase velocities of the modes $m = 1$ and $m = 2$ decrease markedly at low Strouhal numbers.

It is shown in Fig. 2 that the helical disturbance waves amplify and then decay in a manner similar to the plane wave case. The spreading of the disturbances is also similar to that of the plane wave. For high Strouhal numbers the disturbances are confined within the part of the shear layer near the nozzle, whereas for low Strouhal numbers they extend far into the fully developed turbulent region downstream. The measured rms values of the wave disturbances along the jet for a range of Strouhal numbers are shown in Fig. 4 for the $m = 1$ and $m = 2$ modes. Note that the abscissa is in a normalized distance (X/D) St and the ordinate is in a dB unit. All cases show that the waves amplify exponentially in the initial stage, reach a maximum, and then decay gradually farther downstream. For the $m = 1$ mode, except the cases with Strouhal numbers lower than 0.25, some similarities can be observed for the growth and decay of the amplitude profiles. With some scattering, they all reach the same maximum amplitude at about the same normalized distance. For the $m = 2$ mode, however, the regularity of the contours is less pronounced. The peak values of the contours increase steadily with the Strouhal number and approach a plateau at $St = 67$. The peaks of the pressure amplitude for the $m = 2$ modes are always lower than those of the $m = 1$ mode.

The variations of the pressure amplitude across the shear layers of the jet are shown in Fig. 5. The radial traverse was taken at a station where the longitudinal amplitude reached its maximum value. At the centerline of the jet where the radial traverse starts, the amplitude of the pressure wave is very low. The amplitude increases rapidly to a maximum near the center of the shear layer and then decays exponentially as the radial distance increases. For the $m = 1$ mode, except in two cases of

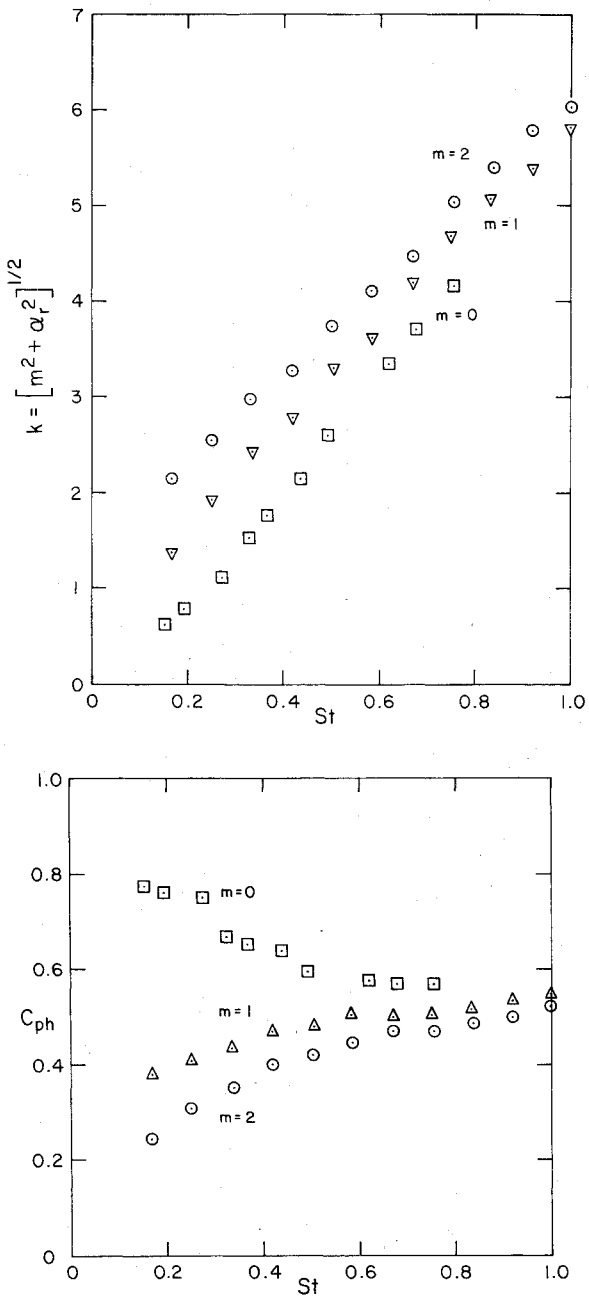

Fig. 3 a) Wave number vs Strouhal number for modes $m = 0, 1$, and 2 b) Phase velocity vs Strouhal number for modes $m = 0, 1$, and 2.

low Strouhal number, the contours show striking similarity in shape. For the $m = 2$ mode, the results are more scattered and less regular. The peak values of the contour again increase with the Strouhal number and flattens off at higher Strouhal numbers. It is interesting to note that for both modes the disturbance does vanish at the center of the jet, as required by the physical consideration of a helical wave.

The direct measurements of the development of the helical disturbance waves in the jet presented here show that the large-scale wavelike eddies in a turbulent jet can have modes higher than $m = 0$, i.e., a plane wave. These results are consistent with Fuchs' experiment, which showed that the turbulence in the jet can be resolved into azimuthal Fourier components and that the first four components dominate.[5]

III. Calculation of Helical Wave Development in a Jet

It has been shown by several authors that the large-scale wavelike eddies in the turbulent jet can be well modeled by the

wave-guide theory of Landahl.[9,10,12,18,19] These theoretical analyses follow closely the nonlinear theory of hydrodynamic stability developed for laminar shear flows. For a highly nonlinear process, an exact analysis is difficult; however, the development of the wave and its interaction with the mean and the turbulent flow can be examined globally by considering the energy transfer in the shear layer. The energy method for the nonlinear stability analysis was first formulated by Stuart.[23] The method was advanced by Ko et al. in an analysis of the nonlinear stability of a laminar wake.[24] Its application to the analysis of stability waves in a turbulent wake was demonstrated by Liu.[25] In a detailed analysis of a plane wave propagating in an axisymmetric turbulent jet, the method was applied by Chan to calculate the growth and decay of the wave. His theoretical results agreed well with experimental data.[20]

A. Formulation

The fundamental equations governing the problem can be derived from the Navier-Stokes equations and the continuity equation. For the present application to an axisymmetric jet, a cylindrical polar coordinate system is used. The physical variables are normalized by R (radius of the jet nozzle) and the velocity U (exit velocity of the jet). In deriving the equations, both the turbulent fluctuation and the wave disturbance are considered to be small compared with the mean flow quantities. Thus the velocity components and the pressure can be split into three components, namely, the steady mean flow, the disturbance wave fluctuation, and the turbulent fluctuations as follows.

$$u=\bar{u}+\tilde{u}+u'$$
$$p=\bar{p}+\tilde{p}+p' \qquad (2)$$

The mean flow equations are derived by first taking the phase average and then the time average of the Navier-Stokes equation. The wave-component equations are then obtained by subtracting the phase-averaged equations from the time-averaged mean flow equations. The kinetic energy equations are derived by multiplying the Navier-Stokes equations by the corresponding velocity components and then taking averages. Boundary-layer approximation is applied throughout the derivation and for turbulent flow, the effect of molecular viscosity is neglected. The flow is considered to be incompressible. The details of the derivation of the equations are given in Ref. 20.

The resulting equations for the present analysis by the energy method are the kinetic energy equations of the mean flow, the turbulent fluctuation, and the wave disturbance

$$\bar{u}\frac{\partial \bar{u}^2/2}{\partial x}+\bar{v}\frac{\partial \bar{u}^2/2}{\partial r}=-(-\overline{\tilde{u}\tilde{v}})\frac{\partial \bar{u}}{\partial r}-(-\overline{u'v'})\frac{\partial \bar{u}}{\partial r}$$
$$+\frac{1}{r}\frac{\partial}{\partial r}\{r\bar{u}[(-\overline{\tilde{u}\tilde{v}})+(-\overline{u'v'})]$$
$$\frac{\partial k}{\partial t}+\bar{u}\frac{\partial k}{\partial x}+\bar{v}\frac{\partial k}{\partial r}=\frac{1}{r}\frac{\partial}{\partial r}[r\overline{v'(p'+k)}]$$
$$+(-\overline{u'v'})\frac{\partial \bar{u}}{\partial r}-\epsilon+\phi$$
$$\frac{\partial q}{\partial t}+\bar{u}\frac{\partial q}{\partial x}+\bar{v}\frac{\partial q}{\partial r}=\frac{1}{r}\frac{\partial}{\partial r}[r\overline{\tilde{v}(\tilde{p}+q)}]$$
$$+(-\overline{\tilde{u}\tilde{v}})\frac{\partial \bar{u}}{\partial r}+\frac{1}{r}\frac{\partial}{\partial r}\left(r\epsilon_t\frac{\partial q}{\partial r}\right)-\phi \qquad (3)$$

where k is the turbulent kinetic energy and q the wave kinetic energy. The cascading process of energy transfer in a turbulent shear flow can now be seen from these equations. The kinetic energy of the mean flow is extracted by the growth of the wave and the production of turbulence as represented by the first two terms at the right-hand side of the mean flow energy equation. These two terms then appear as energy sources in the turbulence and the wave energy equations. The energy in the wave is then transferred further to the turbulence, with the dissipation function ϕ being negative in the wave equation and positive in the turbulence equation. The last step causes the decay of the wave and an increment of the turbulent energy.

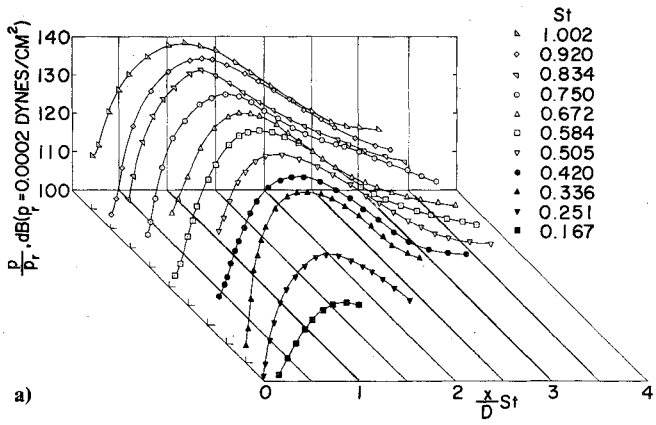

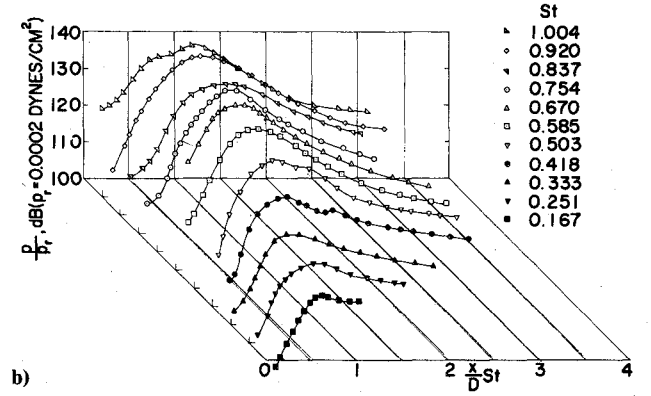

Fig. 4 Pressure amplitude distributions along the jet, a) $m=1$; b) $m=2$.

In the energy method of analysis, these equations are solved by an integral method. The correlation functions required for the integral formulation, those of the mean and the turbulent flows of the jet, are calculated numerically by a finite difference method. Those of the wave fluctuations are obtained from a linear stability theory of a divergent shear flow. The solutions of the mean and the turbulent flows and the solutions of the stability wave required for the evaluation of the correlation functions are now calculated in the following two sections.

B. Mean Flow Calculation

The governing equations for the mean flow of the jet are the continuity and the x momentum equations. As a first approximation, the contributions from the wave disturbance is neglected.

$$\frac{\partial \bar{u}}{\partial x}+\frac{1}{r}\frac{\partial r\bar{v}}{\partial r}=0$$
$$\bar{u}\frac{\partial \bar{u}}{\partial x}+\bar{v}\frac{\partial \bar{u}}{\partial r}=\frac{1}{r}\frac{\partial r(-\overline{u'v'})}{\partial r} \qquad (4)$$

For an axisymmetric jet, the boundary conditions are as

$$\partial k/\partial r=0 \quad \text{at} \quad r=0$$
$$u\to 0 \quad \text{as} \quad r\to\infty \qquad (5)$$

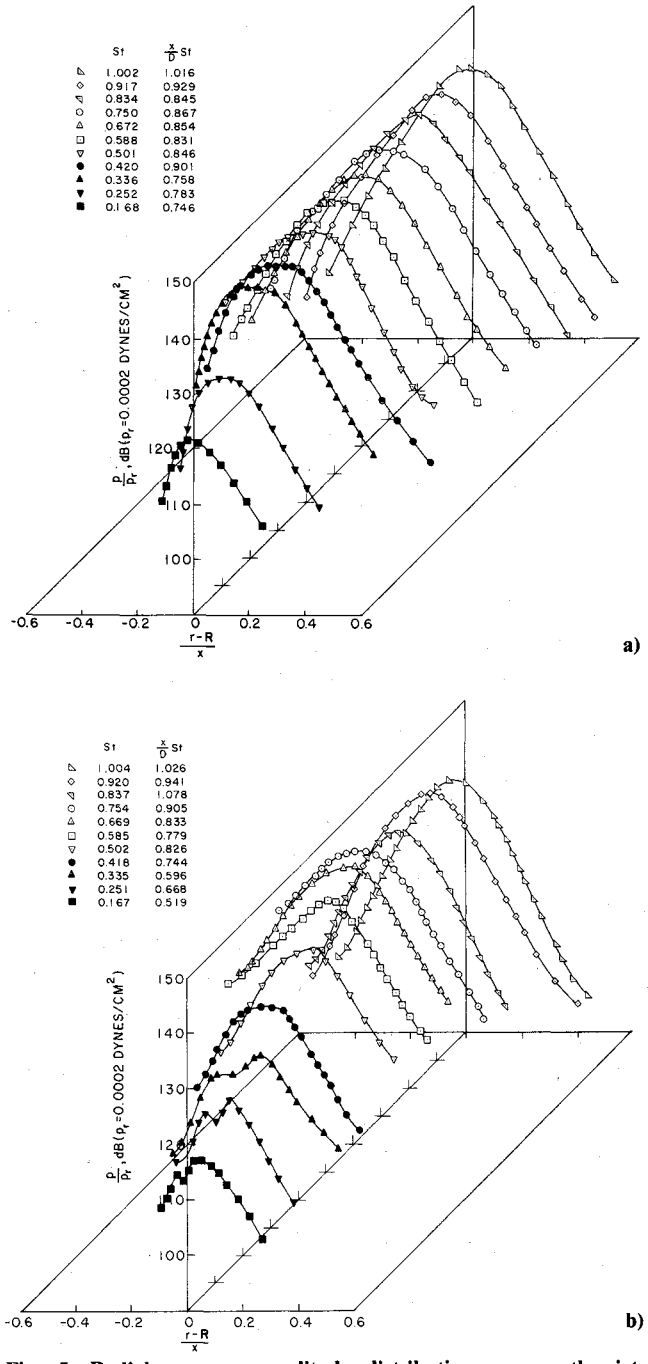

Fig. 5 Radial pressure amplitude distributions across the jet, a) $m=1$; b) $m=2$.

Turbulent kinetic energy distributions inside the jet are required to evaluate the correlation functions for the integral formulation. The turbulent kinetic energy equation, therefore, should be solved simultaneously with the mean flow equations. This equation is written, excluding the wave energy source term, as

$$\bar{u}\frac{\partial k}{\partial x}+\bar{v}\frac{\partial k}{\partial r}=\frac{1}{r}\frac{\partial}{\partial r}[r\overline{v'(p'+k)}]+(-\overline{u'v'})\frac{\partial \bar{u}}{\partial r}-\epsilon \quad (6)$$

with the boundary conditions

$$\frac{\partial k}{\partial r}=0 \qquad \text{at} \qquad r=0$$

$$k\to 0 \qquad \text{as} \qquad r\to\infty$$

Methods for computing free turbulent shear flows are well developed.[26] For the present case, the Prandtl's energy model is adopted.[27] In this model, an eddy viscosity is assumed for the closure of the Reynolds stress, and the turbulent velocity-pressure correlation is taken as a gradient diffusion. This model is written as follows:

$$\epsilon_t=c_l k^{1/2}\ell \qquad -\overline{u'v'}=\epsilon_t\frac{\partial \bar{u}}{\partial r}$$

$$\overline{v'(p'+k)}=\frac{\epsilon_t}{\sigma_k}\frac{\partial k}{\partial r} \qquad \epsilon=c_2\frac{k^{3/2}}{L} \qquad \delta=r_{0.1}-r_{0.9} \quad (7)$$

where c_l and c_2 are empirical constants and σ_k the Prandtl number for the energy equation. Both the length scale ℓ and the dissipation length L are taken to be the thickness δ of the shear layer. The empirical input for the calculation are as follows:

$$c_l=0.05 \quad c_2=1.50 \quad \sigma_k=0.70 \quad \ell=L=\delta$$

A modified von Mises transformation is then applied to the equations. With this transformation the spreading of the jet in the lateral direction is much smaller than that in the physical coordinate and is thus easier to handle in the numerical calculation. The transformation[28]

$$\zeta=\frac{x}{4} \qquad \eta=\left[\int_0^{\eta}\bar{u}r\,dr\right]^{1/2} \quad (8)$$

satisfies the continuity equation automatically

$$2\eta\frac{\partial \eta}{\partial r}=\bar{u}r \qquad 2\eta\frac{\partial \eta}{\partial x}=-\bar{v}r \quad (9)$$

The momentum and the turbulent kinetic energy equations become:

$$\frac{\partial \bar{u}}{\partial \zeta}=\frac{1}{\eta}\frac{\partial}{\partial \eta}\left(r^2\frac{\epsilon_t\bar{u}}{\eta}\frac{\partial \bar{u}}{\partial \eta}\right)$$

$$\frac{\partial k}{\partial \zeta}=\frac{1}{\eta}\frac{\partial}{\partial \eta}\left(r^2\frac{\epsilon_t\bar{u}}{\sigma_k\eta}\frac{\partial k}{\partial \eta}\right)+\epsilon_t\frac{\bar{u}r^2}{\eta^2}\frac{\partial \bar{u}}{\partial \eta}-c_2\frac{4k^{3/2}}{\bar{u}L} \quad (10)$$

with the boundary conditions

$$\frac{\partial \bar{u}}{\partial \eta}=0, \qquad \frac{\partial k}{\partial \eta}=0 \qquad \text{at} \qquad \eta=0$$

$$\bar{u}\to 0, \qquad k\to 0 \qquad \text{as} \qquad \eta\to\infty \quad (11)$$

These equations with the boundary conditions are solved numerically by an implicit finite-difference method. Because of the nonlinear coupling of these two equations, an iterative scheme is used for the solutions. The momentum equation is first integrated with an assumed distribution of turbulent kinetic energy and the resulting velocity distribution is used for the solution of the turbulent kinetic energy equation. The new kinetic energy profile replaces the assumed one and the process continues until the solution converges to satisfy a preset criterion.

The nonlinear momentum equation is first linearized in a form suitable for an iterative calculation. The equation is then written into a finite-difference form resulting in a system of linear algebraic equations that can be solved by an elimination method. The energy equation is weakly nonlinear and can be solved in a similar manner. The details of the numerical analysis are given in Ref. 20.

With the mean flow development of the jet calculated, the resulting mean velocity and kinetic energy profiles are used to

evaluate the correlation functions of the mean and the turbulent flow energy balances for the integral formulation of the nonlinear wave process. The mean velocity profile is also used for the calculation of the wave functions presented in the next section.

C. Stability Wave Calculations

The correlation functions of the wave disturbance are calculated from the linear stability solutions of the local shear flow. This may be the closest approximation that can be assumed without additional information from further experiments or exact nonlinear solutions. The inviscid forms of the linear stability equations are used in the present calculations with the boundary-layer approximation applied to the mean flow velocity components. This is a reasonable approximation for high turbulent Reynolds number flows. The continuity and the momentum equations for the wave disturbances are as follows:

$$\frac{\partial \tilde{u}}{\partial x}+\frac{1}{r}\frac{\partial r\tilde{v}}{\partial r}+\frac{1}{r}\frac{\partial \tilde{w}}{\partial \theta}=0$$

$$\frac{\partial \tilde{u}}{\partial t}+\bar{u}\frac{\partial \tilde{u}}{\partial x}+\tilde{v}\frac{\partial \bar{u}}{\partial r}=-\frac{\partial \tilde{p}}{\partial x}$$

$$\frac{\partial \tilde{v}}{\partial t}+\bar{u}\frac{\partial \tilde{v}}{\partial x}=-\frac{\partial \tilde{p}}{\partial r}$$

$$\frac{\partial \tilde{w}}{\partial t}+\bar{u}\frac{\partial \tilde{w}}{\partial x}=-\frac{1}{r}\frac{\partial \tilde{p}}{\partial \theta} \tag{12}$$

For a turbulent free jet, the shear layer is not parallel to but diverges rapidly away from the jet axis. To take into account the divergency of the shear layer, a transformation of the radial coordinate r is introduced

$$y=(r-1)/b(x)$$

where $b(x)$ is a function of x and can be set equal to the thickness of the shear layer δ. For a single Fourier component of the wave disturbance, a wave form solution is sought

$$\{\tilde{u},\tilde{v},\tilde{w},\tilde{p}\}=\{\hat{u}(y),\hat{v}(y),\hat{w}(y),\hat{p}(y)\}\exp[i(\int\alpha(x)\,dx-\beta t+m\theta)] \tag{13}$$

where $\alpha(x)$ is a complex function of x, the real part being the wave number and the negative imaginary part the amplification rate. β is the circular frequency and m the azimuthal wave number. Substituting Eq. (13) into the governing equations a system of equations depending only on the radial coordinate y is obtained

$$i(A\bar{u}-B)\hat{u}+\hat{v}\frac{d\bar{u}}{dy}=-iA\hat{p}$$

$$i(A\bar{u}-B)\hat{v}=-\frac{d\hat{p}}{dy}$$

$$i(A\bar{u}-B)\hat{w}=-\frac{iM\hat{p}}{r}$$

$$iA\hat{u}+\frac{1}{r}\frac{dr\hat{v}}{dy}+\frac{iM\hat{w}}{r}=0 \tag{14}$$

where $A=\alpha b$, $B=\beta b$, and $M=mb$. The mean flow solutions show that db/dx is an order of magnitude less than unity, thus in deriving Eq. (14) the terms containing db/dx are neglected. For a divergent flow, the quantities $\hat{u}$, etc., should be functions of x and r. The present form is equivalent to taking the first-order term only from a series expansion of $\hat{u}$ in the ascending power of the parameter db/dx. This system of equations resembles closely that of the parallel flow, except that the wave numbers and the frequency are now multiples of the shear-layer thickness $b(x)$. The system of equations can be further simplified to the following form

$$\frac{d\chi}{dy}=-A^2(\bar{u}-c)+\chi\left\{\frac{1}{\bar{u}-c}\left[\frac{A^2+(M^2/r^2)}{A^2}-\frac{d\bar{u}}{dy}\right]+\frac{1}{r}\frac{dr}{dy}\right\} \tag{15}$$

where

$$\chi=-iA(\hat{p}/\hat{v}) \quad \text{and} \quad c=B/A$$

The mean velocity gradients vanish at the edge of the shear layer. Thus the asymptotic solutions provide the required boundary conditions:

$$\chi(y_i)=-A(\bar{u}-c)\frac{I_m(Ar_j/b)}{I_m'(Ar_j/b)} \qquad y\to y_i$$

$$\chi(y_\infty)=Ac\frac{K_m(Ar_\infty/b)}{K_m'(Ar_\infty/b)} \qquad y\to\infty \tag{16}$$

where I_m and K_m are modified Bessel functions. Equation (15) with boundary conditions (16) forms an eigenvalue problem. The local wave number A is the eigenvalue to be calculated for a given frequency B at each station along the jet with a specified mean-velocity distribution. To solve this eigenvalue problem, an iterative scheme is used.[20] By assuming an eigenvalue A, the boundary values can be calculated from Eq. (16), and Eq. (15) is then integrated numerically from both sides of the shear layer toward the center. It is required that, at the point where these integrations meet, the values of χ approaching from both sides should be the same. With the eigenvalue known, the eigenfunctions can be calculated from Eq. (14).

For the present calculation, with the comparison with the experimental data in mind, the frequency β is chosen to be 1.5 ($St=0.477$). The eigenvalue and the eigenfunctions are calculated at a number of stations along the jet axis. The mean velocity gradients at these stations are taken from the solutions of the mean flow obtained in the last section. The local values of the eigenvalues, the wave number α_r and the amplification rate $-\alpha_i$, are plotted against the parameter δ (or b) in Fig. 6. The local values of phase velocity are also shown in the figure. Three azimuthal modes are calculated. In general, the wave number increases steeply with δ, reaching a maximum and then decreases gradually. The amplification rate decreases monotonically except near the very first portion of the jet. As the order of the mode increases, the wave number increases and the corresponding phase velocity decreases. The amplification rate decreases more rapidly for the higher modes and the extent of the jet at which the amplification rate is positive diminishes. The small difference between the wave numbers of the plane wave ($m=0$) and that of the two helical modes is consistent with the experimental data presented in Fig. 3.

D. Energy Integral Method for Nonlinear Wave Process

The nonlinear development of a wave disturbance in the shear layer of a jet is now analyzed by the consideration of the kinetic energy balances in the mean flow, the turbulent fluctuation, and the wave fluctuation. With the mean-flow continuity equation the mean-velocity component $\bar{v}$ can be eliminated from the governing equations (3), which are then integrated across the shear layer. By applying the proper boundary conditions at the edges of the shear layer and noting that the diffusion terms in these equations represent only a

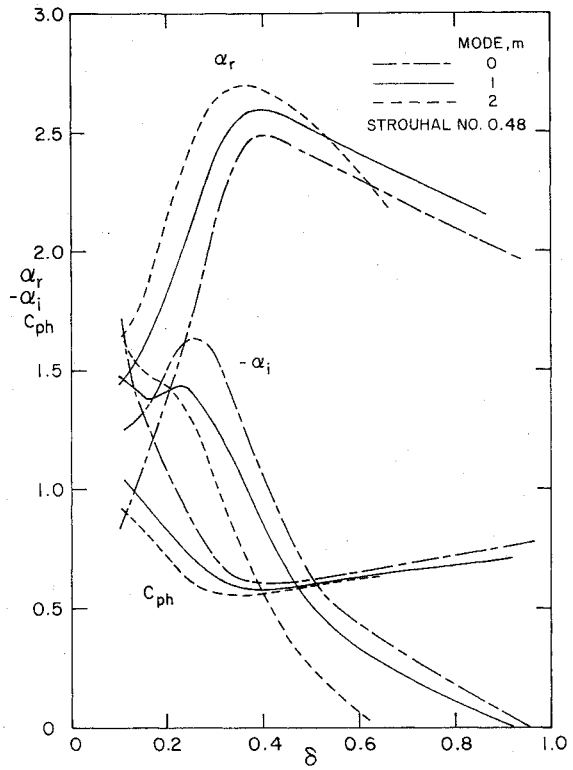

Fig. 6 Local wave numbers, amplification rates and phase velocities as functions of δ for modes $m = 0, 1,$ and 2.

redistribution of energy in the shear layer and thus drop out in the integration, the integral energy equations are

$$\frac{1}{2}\frac{\mathrm{d}}{\mathrm{d}x}\int_0^h \bar{u}^3 r\mathrm{d}r = \int_0^h (-\overline{u'v'})\frac{\partial \bar{u}}{\partial r} r\mathrm{d}r - \int_0^h (-\bar{\bar{u}}\bar{\bar{v}})\frac{\partial \bar{u}}{\partial r} r\mathrm{d}r$$

$$\frac{\mathrm{d}}{\mathrm{d}x}\int_0^h k\bar{u} r\mathrm{d}r = \int_0^h (-\overline{u'v'})\frac{\partial \bar{u}}{\partial r} r\mathrm{d}r - \int_0^h \epsilon r\mathrm{d}r + \int_0^h \phi r\mathrm{d}r$$

$$\frac{\mathrm{d}}{\mathrm{d}x}\int_0^h q\bar{u} r\mathrm{d}r = \int_0^h (-\bar{\bar{u}}\bar{\bar{v}})\frac{\partial \bar{u}}{\partial r} r\mathrm{d}r - \int_0^h \phi r\mathrm{d}r \qquad (17)$$

Three parameters are chosen as unknowns; the shear-layer thickness δ for the mean flow, the averaged turbulent kinetic energy integral k_a for the turbulent flow, and the wave amplitude Q for the wave disturbance. The wave disturbance is assumed to be of the form

$$\{\tilde{u},\tilde{v},\tilde{w},\tilde{p}\} = Q(x)\{\hat{u}(b,y),\hat{v}(b,y),\hat{w}(b,y),\hat{p}(b,y)\}$$
$$\exp[i(\textstyle\int \alpha_r(x)\mathrm{d}x - \beta t + m\theta)] \qquad (18)$$

where $Q(x)$ is the amplitude of the wave. The lateral distribution of the wave functions are assumed to be identical to the linear stability solutions of the local divergent shear layer calculated in Sec. IIIC. The local wave number α_R is also taken from the linear solutions. The form of Eq. (18) also implies that the higher harmonics are neglected.

The averaged turbulent kinetic energy intergral is defined as

$$k_a = \frac{2}{r_2^2 - r_1^2}\int_0^h k(r) r\mathrm{d}r \qquad (19)$$

with the kinetic energy distribution across the shear layer written as

$$k(r) = k_a G(r) \qquad (20)$$

The model of the turbulence for the present formulation is the same as the one used in the mean-flow calculation and

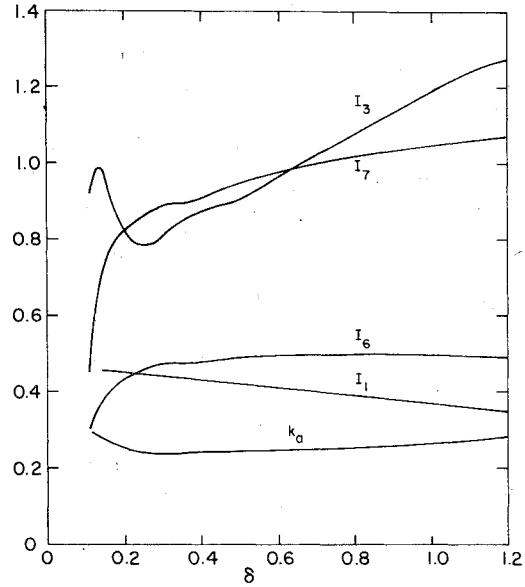

Fig. 7 Correlation functions for the mean flow and the turbulent kinetic energy equations.

given in Eq. (17). With this model, the correlation functions involving only the mean and turbulent flows can be evaluated without difficulty. From the mean-flow solutions of the jet the following integrals

$$I_1 = \int_0^h \bar{u}^3 r\mathrm{d}r$$

$$I_3 = \delta\int_0^h G^{1/2}\left(\frac{\partial \bar{u}}{\partial r}\right)^2 r\mathrm{d}r$$

$$I_6 = \frac{1}{\delta}\int_0^h G\bar{u} r\mathrm{d}r$$

$$I_7 = \frac{1}{\delta}\int_0^h G^{3/2} r\mathrm{d}r \qquad (21)$$

are calculated and plotted in Fig. 7 against the parameter δ. The averaged turbulent kinetic energy integral defined in Eq. (19) is also shown. It is noted that the integral k_a varies only slightly over the range of δ consider. Thus the correlation itegrals can be considered as function of δ only.

Three correlation integrals involve wave functions

$$I_2 = \int_0^h (-\bar{\bar{u}}\bar{\bar{v}})\frac{\partial \bar{u}}{\partial y} r\mathrm{d}y$$

$$I_4 = \int_0^h q\bar{u} r\mathrm{d}y$$

$$I_5 = \int_0^h \phi r\mathrm{d}y \qquad (22)$$

The first two integrals can be evaluated from the stability wave solutions as follows:

$$I_2 \doteq Q^2\left[-\frac{R^2}{2}\int_0^h r(\hat{u}_r\hat{v}_r + \hat{u}_i\hat{v}_i)\frac{\partial \bar{u}}{\partial y}\mathrm{d}y\right] = Q^2 F_2(\delta)$$

$$I_4 = Q^2\left\{\frac{R^2}{4}\int_0^h r[(\hat{u}_r^2 + \hat{u}_i^2) + (\hat{v}_r^2 + \hat{v}_i^2) + (\hat{w}_r^2 + w_i^2)]\bar{u}\mathrm{d}y\right\}$$

$$= Q^2 F_4(\delta) \qquad (23)$$

where the subscripts r and i denote the real and the imaginary parts, respectively. The normalizing factor R^2 in the integrals

is due to the fact that the linear stability solutions are determined up to an arbitrary coefficient of a constant value. In the calculations in Sec. IIIC, this constant is taken to be unity. In the nonlinear analysis, this coefficient is included in the amplitude $Q(x)$. To determine the value of the factor R^2 we set the kinetic energy integral of the wave function equal to $|Q|^2$.

$$|Q|^2=\int_0^h qr\,dy=\frac{Q^2R^2}{4}I_8 \tag{24}$$

where

$$I_8=\int_0^h r[(\hat{u}_r^2+\hat{u}_i^2)+(\hat{v}_r^2+\hat{v}_i^2)+(\hat{w}_r^2+\hat{w}_i^2)]\,dy$$

Thus

$$R^2=4/I_8 \tag{25}$$

The integral I_5 is an integration of the dissipation function ϕ, which expresses the energy transfer from the wave disturbance to the small-scale turbulence and the diffusion due to wave-turbulence interaction. The full expression of this function ϕ is given in Ref. 20. The function consists of terms with phase-averaged second correlations of turbulent fluctuating quantities. Similar to the closure requirement for the time-averaged turbulent quantities, a closure relation has to be assumed for these phase-averaged "Reynolds stresses" in order to complete the formulation. In Ref. 20, following Hussian and Reynolds, these stresses are assumed to be related to the rate of strain of the wave fluctuation, with the local eddy viscosity as the proportional constant.[17] The eddy viscosity is assumed to be identical to that used in the mean flow calculation. Based on this assumption, the dissipation function can be reduced to the following form[20]

$$\phi=\epsilon_t\left\{\left(\frac{\partial\tilde{u}}{\partial x}\right)^2+\left(\frac{\partial\tilde{v}}{\partial x}\right)^2+\left(\frac{\partial\tilde{w}}{\partial x}\right)^2+\left(\frac{\partial\tilde{u}}{\partial r}\right)^2+\left(\frac{\partial\tilde{v}}{\partial r}\right)^2+\left(\frac{\partial\tilde{w}}{\partial r}\right)^2+\left(\frac{1}{r}\frac{\partial\tilde{u}}{\partial\theta}\right)^2+\left(\frac{1}{r}\frac{\partial\tilde{v}}{\partial\theta}\right)^2+\left(\frac{1}{r}\frac{\partial\tilde{w}}{\partial\theta}\right)^2\right\} \tag{26}$$

With the dissipation function ϕ in the form of Eq. (26) the integral I_5 can be evaluated, and the formulation is then complete. The calculation of a plane wave development with this closure assumption shows excellent agreement with the experimental data.[20] An extension of the calculations to higher azimuthal modes, i.e., $m=1$ and $m=2$, however, is not as successful.[29] The dissipation integrals for these cases increase at a tremendous rate along the jet, causing a rapid decay of the wave disturbance. The experimental measurements presented in Sec. II, however, do not indicate this rapid rate of decay. The discrepancy is attributed to the fact that, for the higher azimuthal modes, the calculated azimuthal derivatives which are directly proportional to m are unduly large.

Since the wave-energy dissipation is mainly due to the turbulence-wave interaction, the expression given in Eq. (26), although it may not represent the physical process correctly, shows properly the dimensions of the quantities involved. The contribution for the dissipation by the turbulence is through the eddy viscosity, which is defined by the rms value of the turbulence velocity fluctuation and a turbulence length scale. The contribution from the wave is proportional directly to the wave kinetic energy and inversely to the square of a length scale. Following the dissipation model used in the turbulence calculation (7), the dissipation function ϕ is now given the following form

$$\phi=c_3\frac{k^{1/2}q}{\delta} \tag{27}$$

where the length scale is set equal to the thickness of the shear layer and c_3 is a proportional constant. By comparing results calculated with this model for a plane wave and those calculated with Eq. (26), the constant c_3 is determined to a value of 3.67. This constant, like the other constants c_1 and c_2, should be considered as universal for all other modes.

With the function ϕ in the form Eq. (27), the integral I_5 can be evaluated as

$$I_5=c_3k_a\left\{\frac{Q^2R^2}{4}\int_0^h G^{1/2}[(\hat{u}_r^2+\hat{u}_i^2)+(\hat{v}_r^2+\hat{v}_i^2)+(\hat{w}_r^2+\hat{w}_i^2)]\,r\,dy\right\}=c_3k_aQ^2F_5(\delta) \tag{28}$$

The integrals F_2, F_4, F_5 are calculated from the linear wave solutions and the results are shown in Fig. 8 as function of δ for three modes. The figure shows that the energy production integral F_2 increases rapidly and after reaching a maximum, decreases to zero. As the mode increases, the integral decreases and drops off to zero more quickly. The dissipation integral F_5 varies only slightly over the range considered and the values increase only a small amount as the mode increases.

With the correlation integral evaluated, the energy integral equations (17) can be solved for the parameters b, k_a, and Q. These equations are integrated from an initial station with specified initial conditions. For the present calculations the integration starts at $\chi=0.2$ with the initial conditions as

$$\delta=0.1490 \qquad k_a=0.0257$$

obtained from the mean flow calculations without wave disturbance. In addition, the initial value of the wave kinetic energy integral K_0 is specified and this quantity is related to the strength of the initial wave disturbance.

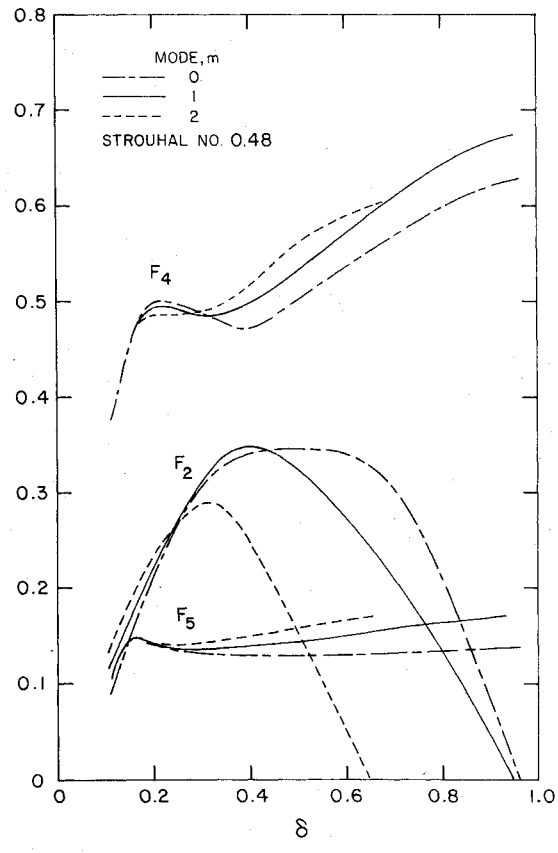

Fig. 8 Correlation functions for the wave kinetic energy equation of modes $m=0$, 1, and 2.

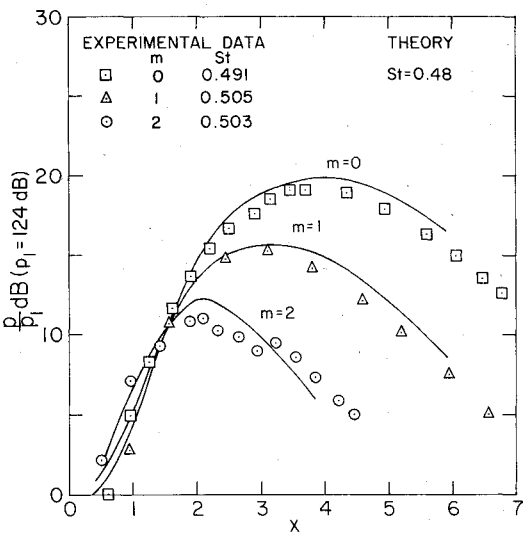

Fig. 9 Calculated growth of the pressure wave amplitudes in comparison with experimental data for modes $m = 0$, 1, and 2.

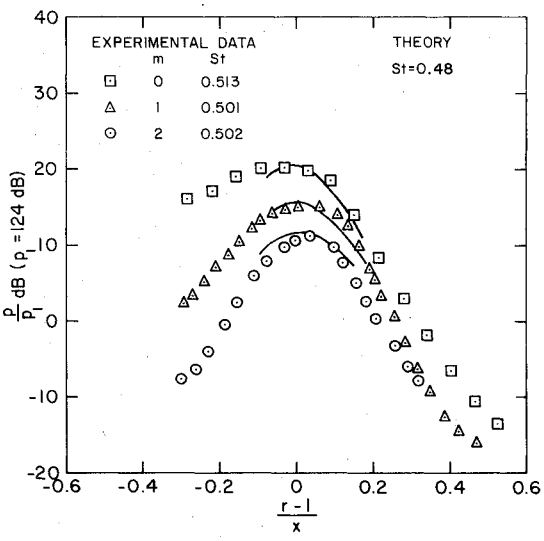

Fig. 10 Calculated radial distribution of the pressure wave amplitudes in comparison with experimental data for modes $m = 0$, 1, and 2.

IV. Results and Discussions

With the method described above the energy transfer in the jet can be calculated in detail. For the initial portion of the jet the production of the wave kinetic energy is much greater than the dissipation. The corresponding pattern for the wave kinetic energy is a rapid increase to a maximum, where production and dissipation are of equal magnitude, followed by a gradual decay.

The wave energy dissipated by the turbulence appears as an energy source to the turbulence itself. For a large wave disturbance, the energy transfer from the wave to the turbulence is of the same order of magnitude as that of the background turbulence. The sharp increment of turbulent energy results in the enhancement of mixing and spreading of the jet.

The growth of the pressure wave in the center of the shear layer, $r = 1$, for all three modes is shown in Fig. 9. The experimental data for $m = 1$ and 2 modes are taken from Sec. II and for $m = 0$ mode from the plane wave experiments.[3] The magnitude of the initial disturbance used in the calculations was set equal to the strength of the forcing induced into the jet in the experimental program. The scale of the pressure ratio is in dB units for convenient comparison with experimental data. For all three modes, the calculated results agree very well with the experimental data over the range considered. Comparisons of the radial pressure distribution data and the calculated results are shown in Fig. 10. The calculated results are again in good agreement with the experimental data for all three modes. The experimental data extend from the potential core to the near-field of the jet, whereas the theoretical results cover only the width of the shear layer.

Both theory and experiment show that the initial amplification of the wave for all three modes is very much the same. However, the maximum of the pressure amplitude decreases as the mode increases due to the lowering of energy production for the higher modes (see Fig. 8). The extent of the wave propagation along the jet is also reduced for the higher modes. The present results are consistent with the experimental observations by Fuchs, that for the turbulence in an axisymmetric jet the first four azimuthal Fourier components dominate and their magnitudes decrease in sequence as the order increases.[5]

In conclusion, we have shown both experimentally and theoretically that an axisymmetric turbulent jet can support in addition to the plane wave mode, a helical wave train with the azimuthal mode equal to or greater than unity. The disturbance wave grows rapidly along the jet to a maximum and then decays gradually farther downstream. The amplitude of the wave decreases as the mode increases and the extent of the wave propagation along the jet is also reduced for the higher modes. The wave numbers in the direction of the jet, however, differ only slightly for all three modes considered. These disturbances of all modes are well modeled by a wave theory in which the local properties of the wave propagation is described by a linear stability solution of a divergent shear flow. The development of the waves along the jet can be calculated by an energy integral method, which is based on the global consideration of the energy transfer taking place in the shear layer between the mean flow, the turbulence, and the wave disturbance.

References

[1] Mollφ-Christensen, E., "Jet Noise and Shear Flow Instability Seen from an Experimenter's Viewpoint," *Journal of Applied Mechanics,* Vol. 34, 1967, pp. 1-7.

[2] Crow, S.C. and Champagne, F.H., "Orderly Structure in Jet Turbulence," *Journal of Fluid Mechanics,* Vol. 48, 1971, pp. 547-591.

[3] Chan, Y.Y., "Spatial Waves in Turbulent Jets," *Physics of Fluids,* Vol. 17, Jan. 1974, pp. 46-53.

[4] Lau, J.C. and Fisher, M.J., "The Vortex-Street Structure of 'Turbulent' Jets, Part 1," *Journal of Fluid Mechanics,* Vol. 67, 1975, pp. 299-337.

[5] Michalke, A. and Fuchs, H.V., "Description of Turbulence and Noise of an Axisymmetric Shear Flow," DLR-FB 74-2, Deutsche Forschungs und Versuchsanstalt für Luft- und Raumfahrt E.V., Institut für Turbulenz-forschung, Berlin, June 1974.

[6] Davies, P.O.A.L. and Yule, A.J., "Coherent Structures in Turbulence," *Journal of Fluid Mechanics,* Vol. 69, 1975, pp. 513-537.

[7] Lilley, G.M., "Generation of Sound in a Mixing Region," Tech. Rept. AFAPL-TR-72-53, Vol. IV, Air Force Aero Propulsion Laboratory, Air Force System Command, Wright-Patterson Air Force Base, Ohio, U.S.A., 1972, pp. 2-97.

[8] Michalke, A., "An Expansion Scheme for the Noise from Circular Jets," Z. Flugwiss, Vol. 20, 1972, pp. 229-237.

[9] Liu, J.T.C., "Developing Large Scale Wavelike Eddies and the Near Jet Noise Field," *Journal of Fluid Mechanics,* Vol. 62, 1974, pp. 437-464.

[10] Merkine, L.O. and Liu, J.T.C., "On the Development of Noise-Producing Large-Scale Wavelike Eddies in a Plane Turbulent Jet," *Journal of Fluid Mechanics,* Vol. 70, 1975, pp. 353-368.

[11] Tam, C.K.W., "On the Noise of a Near Ideally Expanded Supersonic Jet," *Journal of Fluid Mechanics,* Vol. 51, 1972, pp. 69-95.

[12] Tam, C.K.W., "Supersonic Jet Noise Generated by Large Scale Disturbances," *Journal of Sound and Vibration,* Vol. 38, 1975, pp. 51-79.

[13] McLaughlin, D.K., Morrison, G.L., and Trout, T.R., "Experiments on the Instability Waves in a Supersonic Jet and Their

Acoustic Radiation," *Journal of Fluid Mechanics,* Vol. 69, 1975, pp. 73-95.

[14] McLaughlin, D.K., Morrison, G.L., and Trout, T.R., "Reynolds Number Dependence in Supersonic Jet Noise," AIAA Paper No. 76-491, July 1976.

[15] Laufer, J., Kaplan, R.E., and Chu, W.T., "On the Generation of Jet Noise," AGARD Conference Proceeding No. 131 on Noise Mechanisms, 1973.

[16] Landahl, M.T.,"A Wave-Guide Model for Turbulent Shear Flow," *Journal of Fluid Mechanics,* Vol. 29, 1967, pp. 441-459.

[17] Hussain, A.K.M.F. and Reynolds, W.C., "The Mechanics of an Organized Wave in Turbulent Shear Flow," *Journal of Fluid Mechanics,* Vol. 41, 1970, pp. 241-258; "Part 2, Experimental Results," *Journal of Fluid Mechanics,* Vol. 54, 1972, pp. 241-261; "Part 3, Theoretical Models and Comparisons Experiments," Vol. 54, 1972, pp. 263-288.

[18] Morris, P.J., "A Model for the Structure of Jet Turbulence as a Source of Noise," AIAA Paper No. 74-1, Jan. 1974.

[19] Chan, Y.Y., "Spatial Waves in Turbulent Jets, Part II," *Physics of Fluids,* Vol. 17, Sept. 1974, pp. 1667-1670.

[20] Chan, Y.Y., "Nonlinear Spatial Wave Development in an Axisymmetrical Turbulent Jet," Aero Report LR-585, National Research Council Canada, Ottawa, Ontario, April 1975.

[21] Lee, B.H.K. and Payne, L.F., "Turbulence and Wave Measurements in a Subsonic Jet," LTR-HA-22, National Aeronautical Establishment, National Research Council Canada, Ottawa, Ontario, 1974.

[22] Batchelor, G.K. and Gill, A.E., "Analysis of the Stability of Axisymmetric Jets," *Journal of Fluid Mechanics,* Vol. 14, 1962, pp. 529-551.

[23] Stuart, J.T., *Hydrodynamic Stability in Laminar Boundary Layers* (L. Rosenhead, editor), Oxford University Press, Oxford, 1963.

[24] Ko, D.R., Kubota, T., and Lees, L., "Finite Disturbance Effect on the Stability of a Laminar Incompressible Wake Behind a Flat Plate," *Journal of Fluid Mechanics,* Vol. 40, 1970, pp. 315-341.

[25] Liu, J.T.C., "Nonlinear Development of an Instability Wave in a Turbulent Wake," *Physics of Fluids,* Vol. 14, Nov. 1971, pp. 2251-2257.

[26] "Free Turbulent Shear Flows," Vol. 1, Conference Proceedings SP-321, NASA, 1973.

[27] Launder, B.E., Morse, A., Rodi, W., and Spalding, D.B., "Prediction of Free Shear Flows – A Comparison of the Performance of Six Turbulent Models in Free Turbulent Shear Flows," NASA SP-321, 1973, pp. 361-442.

[28] Sinha, R. Fox, H., and Weinbergen, L., "An Implicit Finite Difference Solution for Jet and Wake Problems," ARL-70-0025, Aerospace Research Laboratory Office of Aerospace Research, United States Air Force, Wright-Patterson Air Force Base, Ohio, 1970.

[29] Chan, Y.Y., "Spatial Waves of Higher Modes in an Axisymmetric Turbulent Jet," *Physics of Fluids,* Vol. 19, Dec. 1976, pp. 2042-2043.

[30] Laufer, J. and Browand, F., "The Role of Large Scale Structure in the Initial Development of Circular Jets," Fourth Bi-Annual Symposium on Turbulence in Liquids. Rolla, Mo., Sept. 1975.